COBEM 2023 27TH INTERNATIONAL CONGRESS OF MECHANICAL ENGENEERING

ABCM Brazilian Society of Mechanical Sciences and Engineering
27th ABCM International Congress of Mechanical Engineering
December 04-08, 2023, Florianópolis-SC, Brazil

COB-2023-0642
THE INFLUENCE OF VANELESS ANNULAR PASSAGE IN THE PERFORMANCE OF A CENTRIFUGAL COMPRESSOR WITH VANED DIFFUSER

Rafael Eller
Elóy Gasparin
Sao Paulo State University. Brazil Sul Avenue -56, 15385-000, Ilha Soleira/São Paulo – Brazil.
rafael.s.eller@unesp.br
eloy.gasparin@unesp.br

Jurandir Itizo Yanagihara
University of Sao Paulo – Reitoria St, Cidade Universitária St, 374 - Butantã, São Paulo - SP, 05508-220.
jiy@usp.br

Leandro Salviano
Sao Paulo State University. Brazil Sul Avenue -56, 15385-000, Ilha Soleira/São Paulo – Brazil.
leandro.salviano@unesp.br

Abstract. *Centrifugal compressors are widely used in industrial applications, including power generation, transportation, and the oil industry. This study focuses on investigating the influence of the vaneless annular passage in the performance of a centrifugal compressor with a vaned diffuser. Computational Fluid Dynamics (CFD) simulations were employed to analyze flow phenomena and their effects on loss sources and performance. The diffuser, responsible for converting impeller kinetic energy into static pressure, plays a crucial role in optimizing compressor efficiency. Different types of vaned diffusers were examined, and the impact of varying the diffuser inlet and impeller outlet radius ratio (R3/R2) was studied. A preliminary geometry was created using a 1D code design, and a mesh was generated using GCI methods. The 3D model was validated and simulated using Ansys 19.0 software. Metrics such as pressure recovery and isentropic efficiency were evaluated to determine optimal design alternatives. The findings contribute to the understanding and improvement of centrifugal compressor performance, particularly regarding the vaneless annular passage. This research demonstrates the importance of 3D-CFD modeling in capturing relevant phenomena that one-dimensional models fail to predict.*

Keywords: *Centrifugal compressor; Vaned Diffuser; Vaneless annular passage; CFD.*

1. INTRODUCTION

The fast industrial development of recent decades has led to increased consumption of goods and materials, resulting in greater utilization of natural resources and a rise in greenhouse gas emissions. In response to this pressing issue, substantial efforts have been made to mitigate these impacts and foster a more sustainable society in terms of production, consumption, and overall development. Various methodologies and techniques have been developed to address these challenges. The concentration of greenhouse gasses, particularly CO2 and CH4, has significantly increased in the atmosphere, necessitating the exploration of new strategies to tackle this problem. The escalating levels of these gasses are causing adverse climate changes, resulting in social and environmental repercussions. According to estimates from the Intergovernmental Panel on Climate Change (IPCC) (Kim, 2020), the average global temperature is projected to rise by 3.5°C by 2100. One of the strategies being pursued involves the capture and storage of greenhouse gasses in reservoirs, enabling their reuse in industrial processes and preventing their release into the atmosphere. Another emerging approach is injecting greenhouse gases into depleted coal and oil reservoirs or reinjecting them into active reserves to enhance oil production and address erosion issues in these areas (Godec et al., 2011). It is estimated that worldwide, this technique has the potential to produce approximately 470 billion barrels of oil and store 140 gigatons of CO2 (Godec et al., 2011).

To safely store gases underground, various engineering processes are employed to prevent their abrupt release into the atmosphere (Roddy, 2010). Depleted oil and natural gas reserves are the primary candidates for receiving gases from industrial operations. The injection of CO2 into active oil fields and reserves, known as Enhanced Oil Recovery (EOR), is estimated to be applicable in 80% of global reservoirs (Roddy, 2010). Another alternative method is Enhanced Coal Ced Methane (ECBM), which involves storing CO2 and methane in coal seams and offers additional benefits for methane production (Roddy, 2010). The process of capturing and storing CO2 and CH4 involves extracting these gases from industrial emissions, such as power plants, steel mills, and cement factories, followed by compression and transportation through pipelines to the desired reservoir, whether natural or artificial.

In the compression and transportation stages, centrifugal compressors play a crucial role, necessitating geometric optimization to maximize their efficiency. In these applications, the compressed gasses (CO2 or CH4) reach a thermodynamic state where the temperature and pressure are close to or above the critical point, creating a supercritical gas region where the distinction between liquid and gas behavior becomes challenging. This introduces instabilities, where even slight changes in pressure or temperature can cause significant variations in thermodynamic properties. Supercritical CO2 (sCO2) compressors offer immense potential in this context, as they operate using the Brayton cycle to generate energy, capitalizing on the "liquid-like" thermodynamic behavior of CO2 at low temperatures, thereby improving thermal efficiency.

Centrifugal compressors are composed of three main components: The impeller, the diffuser and the volute or returning channel. The component located between the impeller and the volute is the diffuser. It converts a part of the remaining kinetic energy that leaves the impeller at high speed, into potential energy, i.e., static pressure by gradually decreasing the velocity of the fluid (Aungier, 2000), (Sorokes and Kuzdzal, 2010). Diffusers are one of the most important aerodynamic components in centrifugal compressors, so it is no surprise that they have evolved substantially since the early days of centrifugal compressor use, they can be either vaneless or vaned (Sorokes and Kuzdzal, 2010). There are also hybrid versions of these diffusers including wedge, channel, and pipe (Aungier, 2000). Vaneless diffusers are composed of a channel through which the fluid flows after leaving the impeller, as seen in Figure 1, and are known to have lower efficiency due to interaction effects with the flow from the impeller (Aungier, 2000). Although they offer lower pressure recovery due to these interaction effects, they can work with higher flow rates, since there are no vanes to interfere with the flow (Sorokes and Kuzdzal, 2010). Vaneless diffusers were widely used on older centrifugal compressors because of their simple design, the parallel walls were easy to construct and fabricate, leading to a finer surface finish, improving component performance. However, limited peak pressure recovery (usually below 50%) restricted the level of efficiency possible for this component (Sorokes and Kuzdzal, 2010).

One of the main differences between vaneless diffusers and vaned diffusers is that vaned diffusers allow for a greater pressure gain in the same radius ratio, the vanes form channels that allow flow passage through and causes high decrease in swirl than what is attainable only by reducing circumferential velocity in the channel of a vaneless diffuser. Hence comes one of the greatest vaned diffusers advantages, since for projects that occupy less space to reduce the use of materials and impacts, diffusers with a smaller radius are preferable, therefore, vaned diffusers are preferred over vaneless diffusers. However, although vaned diffusers occupy smaller spaces and generate greater pressure recovery, this comes at a cost in the form of reduced operating range. For high flow rates, vaned diffusers may choke in the throat region located between the vanes, whereas at low flow rates, the diffuser may stall, which generates instabilities in the operation and eventually surge (Casey and Robinson, 2021).

Vaned diffusers are composed of an initial region formed by a channel, named vaneless annular passage, and a region with blades (vanes). There are several types of vaned diffuser geometries in use on the market, each with its singularities, however, there is a general way of categorizing this equipment, being classified as cascade diffusers and channel diffusers. Channel diffusers have more flat wedge-shaped vanes and cascade diffusers have a more airfoil-oriented shape. Figure 1 illustrates some of the geometry variations that are included in this categorization. The choice of which vaned diffuser to use will generally depend on the objectives and limitations of the project or the company, that is, manufacturing cost, final equipment assembly, machinery available for manufacturing and the history of empirical studies and data obtained by the company (Aungier, 2000).

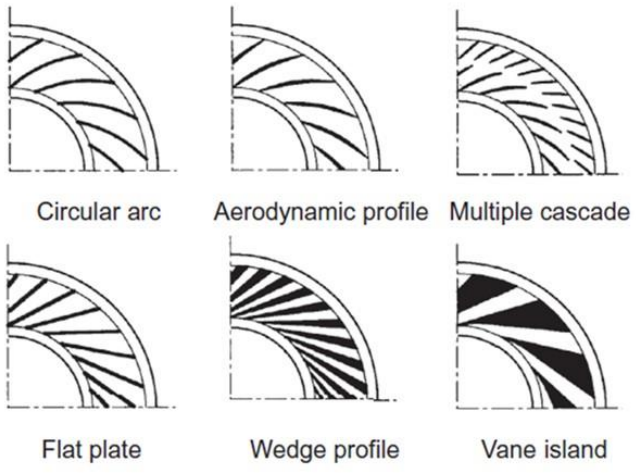

Figure 1. Various cascade diffusers and channel diffusers profiles (Casey and Robinson, 2021).

This component is therefore of great importance and is the subject of several studies in literature. However, designing high efficiency equipment is necessary and a difficult task since the flow has complex phenomena such as adverse pressure gradients, recirculation, and jet-patterns (Denton, 1993). For the diffuser is no different, and an efficient design is always desirable, which is why several works focus on the optimization of this component. Many methods used are based on experimental data that are extremely dependent on the geometry of the compressor used in the experiment. To avoid this dependency, it was necessary to seek alternative methods, which have emerged due to computational development in recent decades. Numerical solutions, specifically using CFD codes such as RANS, based on the Navier-Stokes equations, have shown that it is possible to obtain high performance from preliminary geometries developed by literature methodologies (Ameli et al., 2019), (Lee et al., 2000), (Shaaban, 2015).

Niu et al. (2022) conducted a study on the effects of a non-axisymmetric volute on rotating stall. Although they used a vaneless diffuser instead of a vaned one, they initiated a discussion about flow phenomena in the annular passage. They discovered that the entire annular region experiences stall simultaneously with a decrease in flow rate, with stall cells initiating in a specific portion of the annular passage radius (Niu et al., 2022). This discussion highlights the importance of stall as a phenomenon related to vaneless annular passages, including vaneless diffusers.

Wet et al. (2012) investigated the performance of a turbocharger compressor. They conducted tests on a prototype compressor and observed that a rotating stall occurred in the diffuser section before the designed higher pressure ratio could be achieved. They employed the method proposed by Aungier (2000) regarding the vaneless annular passage between the impeller outlet and the vaned diffuser inlet and concluded that the diffusion process along the passage is mainly governed by the conservation of angular momentum and the increase in flow area due to an increase in radius (Wet et al., 2012), (Casey and Robinson, 2021). They recommended a redesign of the diffuser section based on the results obtained from 1-D and 3-D modeling.

Following this brief overview of relevant literature references and the importance of studying aspects of vaned diffusers, this work aims to investigate the influence of the vaned diffuser inlet radius, which determines the size of the vaneless annular passage, on performance and flow phenomena using 3-D modeling based on the RANS methodology and grid independence techniques.

2. METHODOLOGY

The first step involves obtaining the geometry, which consists of an impeller and a vaned diffuser. A preliminary geometry will be generated using a Python-based 1D code that utilizes correlations and design studies from Aungier (2000) work. This preliminary geometry data will then be inputted into ANSYS BladeGen software to create the vanes and subsequently exported to ANSYS Design Modeler for parameterization. To create different geometries for the vaneless annular passage, the radius ratio of the region is selected as a parameter for this study. Additionally, the blade generation software is crucial, as it determines the angle, thickness, and positions of the leading and trailing edges of the blades. In this study, the original angle, thickness, and leading-edge position will remain constant, along with the length of the diffusion channel. Therefore, the radius ratio, denoted as "λ", is parameterized as shown in Figure 2.a, and its range of variation is specified in Table 1. The angle and thickness definitions are illustrated in Figure 2.b.

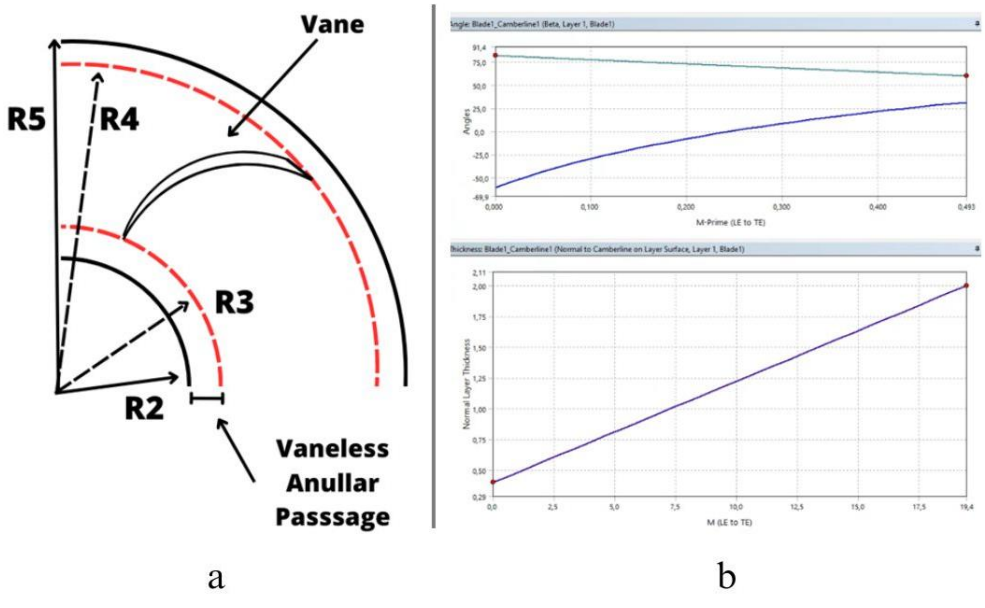

Figure 2. Geometric parameterization scheme (a) and blade angle-thickness definition (b).

Table 1. Vaneless Annular passage (λ) variation ranges.

Vaneless Annular passage range				
λ	1,1	1,2	1,3	1,4

A preliminary geometry is depicted in Figure 3, which showcases the periodic computational domain utilized to reduce computational costs compared to simulating the entire compressor domain. The equivalence theorem leverages the symmetrical parts of the domain (periodic domain) as they are assumed to exhibit similar behavior. Therefore, the solution obtained for one part can be extrapolated to the others, resulting in a complete solution with lower computational expenses. ANSYS Design Modeler was employed as the software for parameterization and geometry construction, using the geometric characteristics obtained from the 1D code as a foundation, through importation via ANSYS Turbogrid software. This specialized software facilitates the creation of meshes for turbomachines, enabling rapid mesh construction and discretization of the periodic domain. It also analyzes important mesh quality parameters such as y+ and Aspect ratio.

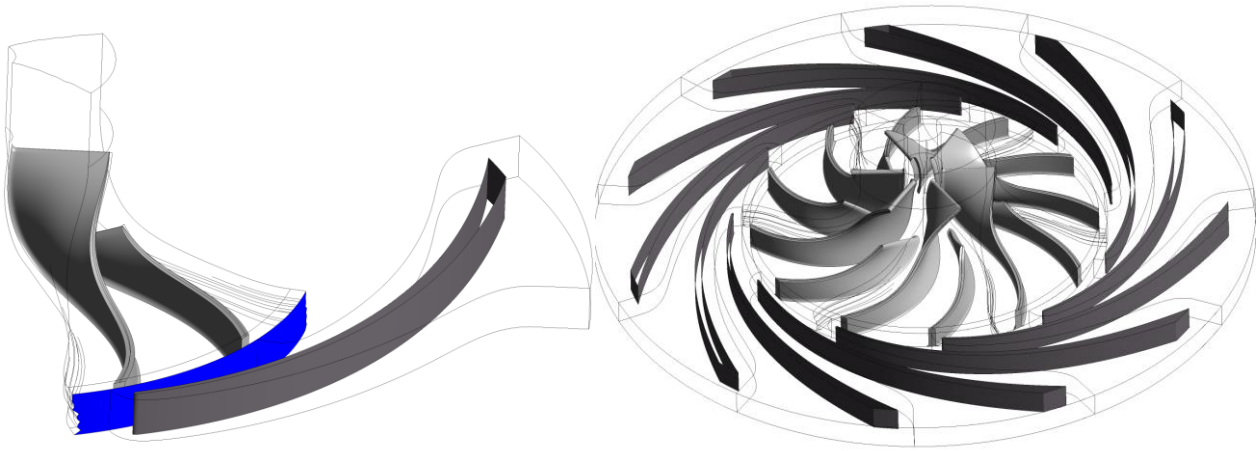

Figure 3. Geometry of impeller-diffuser model.

The boundary and operating conditions are summarized in Table 2. The walls were assumed to exhibit a no-slip and smooth condition, as this configuration has undergone appropriate numerical validation, (Ameli et al., 2018), (Hosangadi et al., 2018). Convergence criteria were established based on the Root Mean Squared (RMS) residuals of all equations and the average standard deviation of the isentropic efficiency. The solution is considered converged when the RMS residuals reach 10^{-6} or when the standard deviation of the isentropic efficiency from the last 20 cumulative iterations reaches 10^{-4}. The rotational speed and inlet pressure are determined through the 1D analysis, while the mass flow rate is defined by the experimental setup conditions.

Table 2. Operational and boundary conditions.

Operational and Boundary conditions	**Values**
Rotating velocity	50000 rpm
Mass flow	3,5 kg/s
Inlet Pressure	7,7 Mpa
Inlet Temperature	313,2 K
Turbulent Intensity	5%
Blade-Shroud gap	0,25 mm
Wall condition	Smooth and non-slip

The S&W equation of state implemented using the CoolProp library (Bell et al., 2014) was used to appropriately write an RGP file for sCO2 that can be read by the ANSYS CFX solution.

The numerical analysis in this project considers steady state, with supercritical CO2, compressible, turbulent, and three-dimensional flow in a periodic computational domain initially with mixing planes approach in impeller-diffuser's interface. The software used for the simulation is ANSYS CFX, recognized as a great software for turbomachinery applications and widely used in industry and literature. It allows importing the mesh generated in ANSYS Turbogrid, setting boundary conditions, and solving the governing equations that models the flow:

Continuity:

$$\nabla\cdot(\rho U) = 0 \quad (1)$$

Momentum:

$$\nabla\cdot(\rho U \times U) = -\nabla p + \nabla\cdot\tau + S_M \quad (1)$$

Total energy:

$$\nabla\cdot(\rho U I) = \nabla\cdot(\lambda\nabla T) + \nabla\cdot(U\cdot\tau) + U\cdot S_M + S_E \quad (3)$$

Where τ is the stress tensor, I is the rothalpy and, according to the rotating frame of reference system implemented in ANSYS CFX, composed by centrifugal forces (S_{cfg}) and Coriolis acceleration (S_{cor}):

$$I = h_{stat} + 1/2\, U^2 + \omega^2 R^2 \quad (4)$$

$$S_M = S_{M,rot} = S_{cfg} + S_{cor} \quad (5)$$

$$S_{cor} = -2\rho\,(\omega \times U) \quad (6)$$

$$S_{cfg} = -\rho\,\omega \times (\omega \times r) \quad (7)$$

Since the vaned diffuser is a static component, when simulating at this component, the terms in equations 5 to 7 are considered 0, since there is no rotational movement, only the fluid passage through the channel and vanes.

The SST-K-ω turbulence model is used, which alternates between the classical k-ω model for the innermost part of the boundary layer and the standard k-ε model for the remaining parts of the boundary layer and free flow, representing well the effect of turbulent shear stress (Menter, 1993). Such characteristics make this model robust and accurate for problems with high adverse pressure gradients, which are present in centrifugal compressor's flow (Casey and Robinson, 2012) and therefore it is widely used in CFD modeling of such equipment (Ameli et al., 2019), (Bourgeois et al., 2011), (Kim et al., 2010).

To assess grid independence, the Grid Convergence Index (GCI) method is used, known as a robust method to ensure grid independence (Celik et al., 2008). This method uses a refinement factor as a function of fine mesh element's number $n_{(n+1)}$ and coarse mesh elements number n_n defined as:

$$r = (n_{(n+1)}/n_n)^{(1/3)} > 1{,}3 \quad (8)$$

The GCI results are shown in Table 3:

Table 3. GCI Results.

GCI	V	Cells	r	η_S	η_p	W [Watts]	P_r
Coarse	4.978E-6	3451103	-	83.9043	83.9043	585195	1,5189
Medium	4.996E-6	1526721	1.331	84.3023	84.3023	587483	1,5249
Fine	5.007E-6	648166	1.314	84.4715	84.4715	594279	1,5322
GCI32(%)				0,372	0,387	0,316	1,270
GCI21(%)				0,100	0,111	0,339	0,967

GCI results shows that the medium mesh can be used for the application, since the maximum error is in order of 1%.

3. RESULTS AND DISCUSSION

In this section, various performance parameters commonly used in centrifugal compressor design studies are presented and discussed. The focus is on isentropic efficiency, pressure recovery, and required power, aiming to determine the need for further investigations.

Figure 4 illustrates the isentropic and polytropic efficiency plotted against the vaneless annular passage sizing ratio, represented by λ. The highest efficiency values are observed at λ = 1.01, which represents the lower limit of our analysis. The efficiency reaches its lowest point between λ = 1.10 and λ = 1.15. Surprisingly, the efficiency starts to increase again until it reaches a second peak at λ = 1.20, which corresponds to the upper limit of our analysis. These findings suggest

that using smaller vaneless annular passages may lead to higher efficiencies at the peak. It also indicates that the vaneless annular passage itself could be a source of losses in the current centrifugal compressor geometry. By reducing its area, these losses can be mitigated. However, it is worth noting that the efficiency rises again after reaching the minimum value between $\lambda = 1.10$, which raises questions since enlarging the vaneless annular passage would be expected to increase losses. This trend suggests the presence of other factors influencing efficiency, necessitating further investigations. To explore the efficiency trend in more detail, additional simulations could be conducted for higher λ values to investigate if efficiency reaches a maximum. However, there is a limitation in this regard. The vane profile is influenced by multiple parameters, including angle and thickness distribution, leading edge, and trailing edge position. By varying the leading-edge radius R_3 through the λ factor, changes in the vane profile shape occur. To specifically focus on the vaneless annular passage, the authors attempted to minimize significant alterations to the vane shape. Beyond $\lambda = 1.40$, the vane shapes deviate considerably from the original $\lambda = 1.1$ configuration, which would introduce other parameters outside the scope of this investigation. The lower limit of the λ range is also determined by numerical limitations of the software used, as it cannot generate geometry and meshes below $\lambda = 1.03$ threshold. Hence, the authors selected the lowest attainable $\lambda = 1.1$ value.

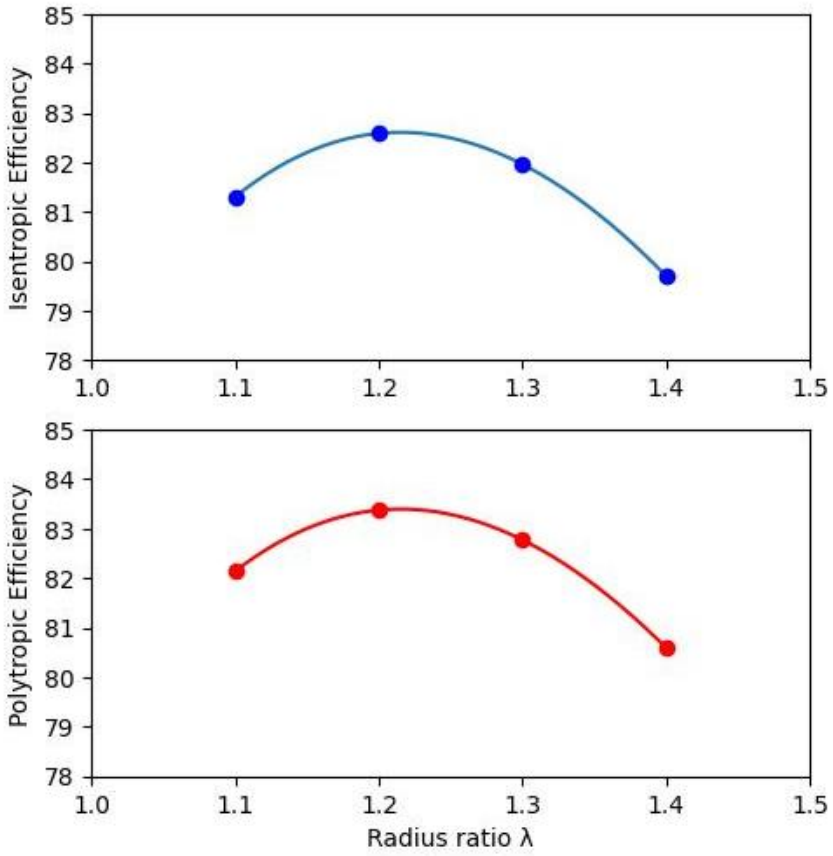

Figure 4. Isentropic efficiency values plotted versus the λ radius ratio.

After analyzing the isentropic efficiency behavior, the pressure ratio is evaluated by plotting the simulated values against the λ ratio. Figure 5 illustrates the pressure ratio (P_r) for each λ ratio value. Its noteworthy that the pressure ratio has a slight change someway like the efficiency behavior. However, the error due to the grid variation indicates that this change is insignificant since the biggest difference is noted taking $\lambda = 1.3$ and $\lambda = 1.4$, exhibiting pressure ratio values of 1.518 and 1.502 respectively, which gives a difference of 1%, same order as the GCI% in Table 3. Thus, we conclude that the change in annular vaneless passage size does not significantly impact the Pressure ratio. This is interesting when returning to the efficiency behavior, since a maximum is reached at $\lambda = 1.2$, and this maximum does not jeopardize the pressure ratio at same radius ratio, meaning that the highest efficiency level does not impact in pressure ratio level, which is important to centrifugal compressors applications.

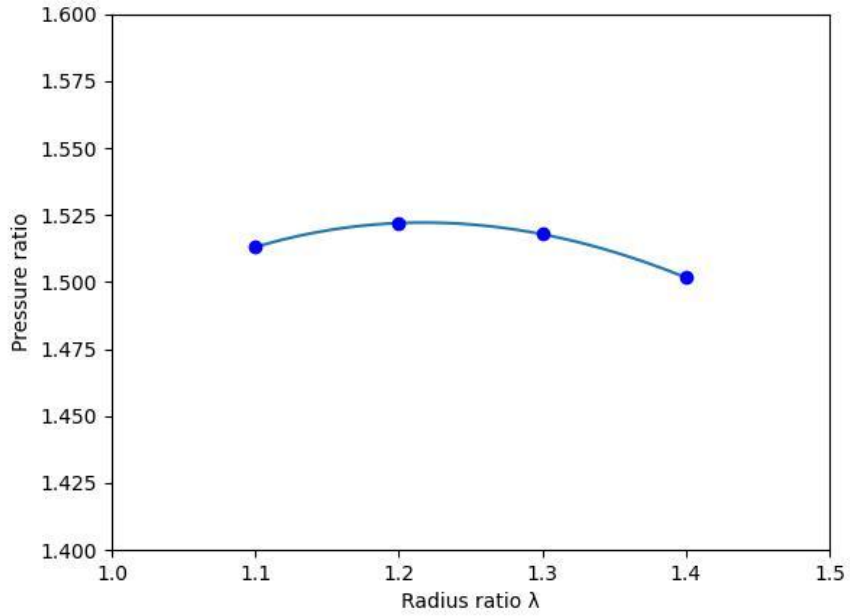

Figure 5. Pressure ratio values plotted versus the λ radius ratio.

Furthermore, it is essential to consider the required power for compressor operation. Figure 6 presents the required power obtained from the simulations plotted against the investigated λ radius ratio values. The figure shows that the required power has a slight rise behavior. However, the error due to the grid variation indicates that this change is insignificant since the biggest difference is noted taking λ = 1.1 and λ = 1.2, exhibiting required power values of 59215.8 and 59242.3 respectively, which gives a difference of 0.04%, below the GCI% in Table 3. Thus, we conclude that the change in annular vaneless passage size does not significantly impact the required power. This is interesting when returning to the efficiency behavior, since a maximum is reached at λ = 1.2, and this maximum does not increase the required power at same radius ratio, meaning that the highest efficiency level does not impact in the required power needed to reach it.

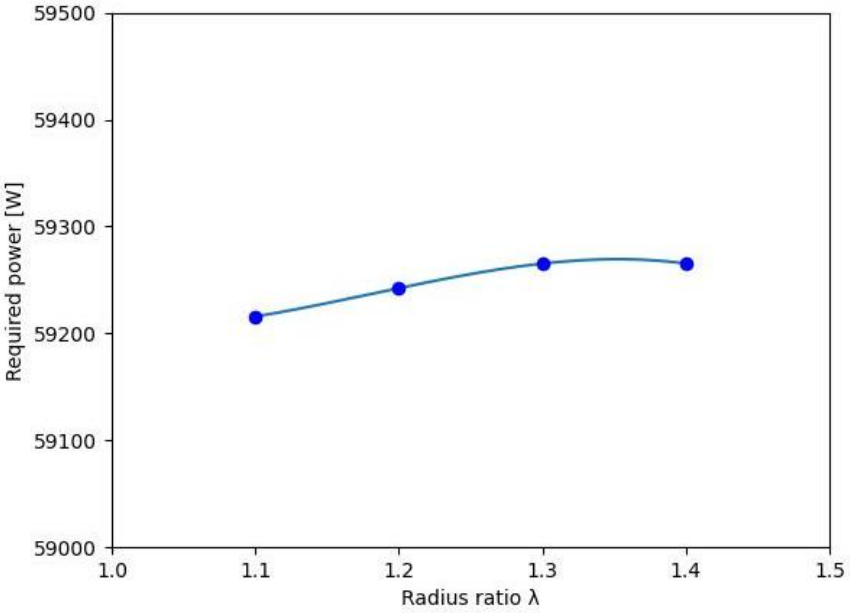

Figure 6. Required Power versus the λ radius ratio.

Based on this discussion, as an initial investigation, it can be concluded that the dependence of vane shape on the leading-edge radius, which also controls the sizing of the vaneless annular passage, may contribute to rise in efficiency. Changes in the vane shape could potentially lead to loss mitigation in the vane region, thus further investigations are needed. To further investigate this aspects, 3D-CFD simulations results were post-processed, using Ansys CFD Post

software, and displayed in the form of the velocity field and velocity vectors shown in the geometries obtained by varying the λ radius ratio. Results are shown in Figure 7.

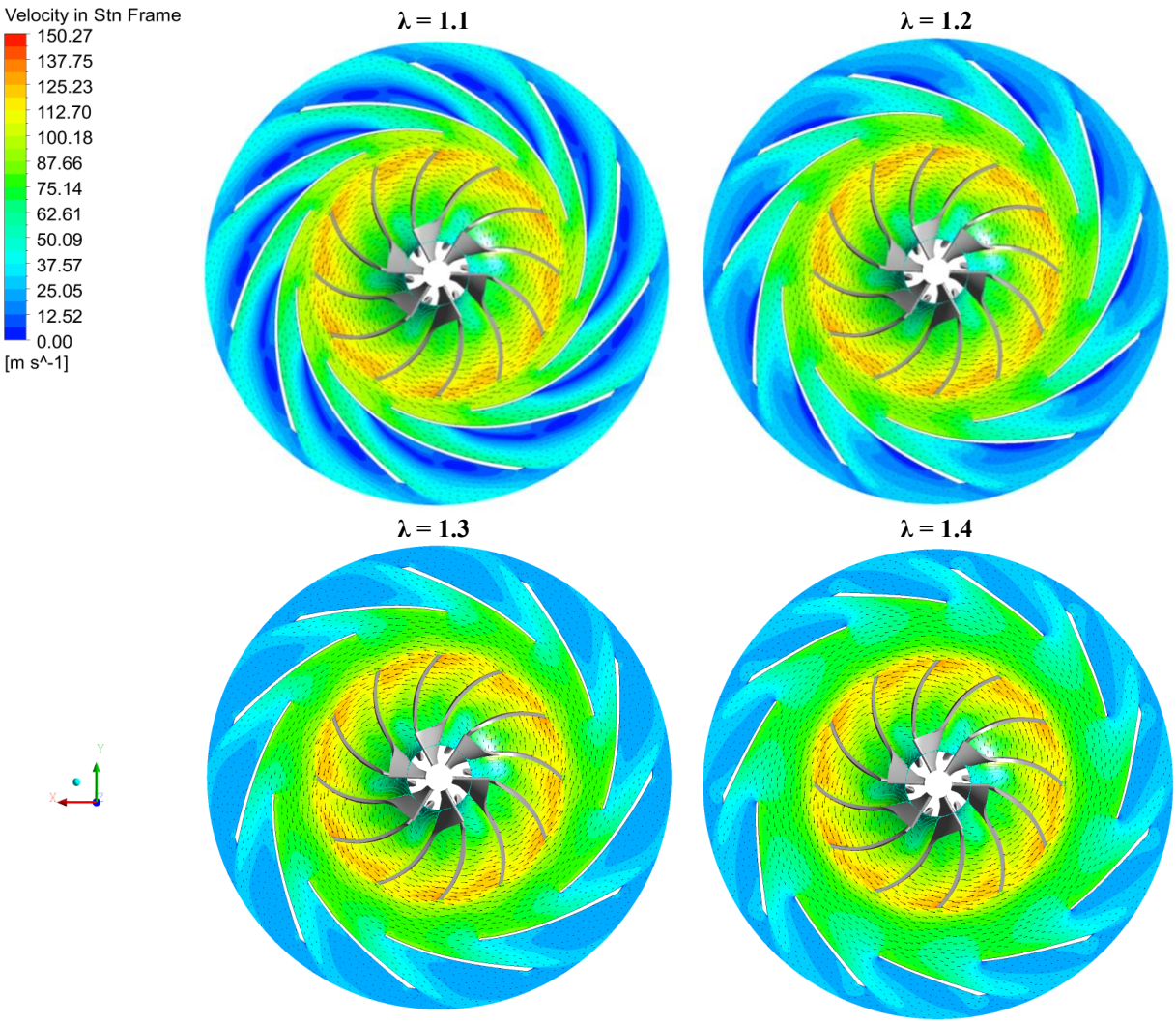

Figure 7 - Velocity Field and Vectors shown in each λ radius ratio geometry.

By analyzing the results in Figure 7, it is possible to observe that the recirculation zones present in vane's surface is reduced by vane shape changing due to λ radius ratio increase, which not only pushes the vane leading edge position in the diffuser, but also deforms the vane shape. Another aspect presented by λ variation is that the velocity zone at the vaneless annular passage become more present, indicating that the fluid is in fact being accelerated at this portion. However, the change in vain shape also changes the fluid deviation through the vane tandem cascade. This impacts the vane cascade mechanism, which is responsible for reducing the velocity swirl component (Aungier, 2000). The fluid guidance along the vanes is another important factor that impacts the diffuser efficiency since the idea is reduce swirl to recover pressure levels and directs the flow to the Volute or returning channel. Therefore, when observing the shape differences in λ = 1.1 and λ = 1.4 geometries it can be concluded that the fluid guidance is jeopardized by the vane shape in λ = 1.4, which explains the lower efficiency level observed in Figure 4.

Comparing the λ = 1.1 geometry with the λ = 1.2 geometry, which has the highest efficiency level observed in Figure 4, the recirculation zone decreases, which means that the vane throat zone is lower. The vane throat zone is an important aspect in vaned diffusers and is recognized as a main source of losses, influencing the vaned diffuser efficiency. It is defined as the region formed between two vanes with the boundary layer separation (Aungier, 2000). Therefore, the optimal behavior of the λ = 1.2 geometry is explained by the vane throat and recirculation zone reduction, and the flow guidance observed through the vanes. These assumptions are reinforced by comparing the λ = 1.2 geometry with the λ = 1.3 one, since it represents the second-best efficiency level observed in Figure 4. By doing this, it is possible to conclude that the λ = 1.3 geometry presents similar characteristics than the 1.2 geometry. However, the optimal case presented better flow guidance than the λ = 1.3 geometry, as observed along the vane regions.

Finally, the pressure contours are plotted for post-processed simulation results investigation. These results are shown in Figure 8 for λ radius ratio variation geometries.

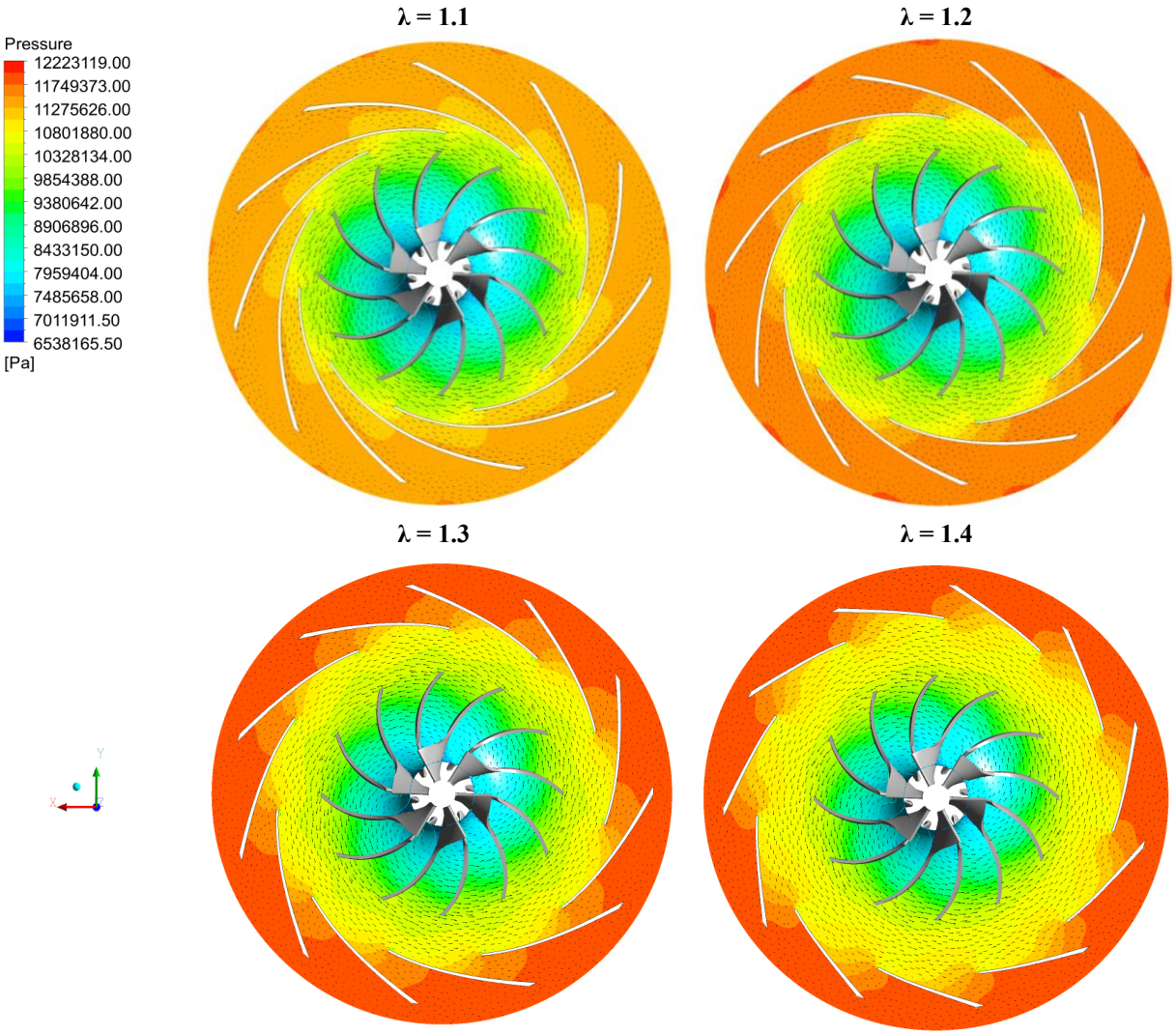

Figure 8 - Pressure contour field and velocity vectors shown in each λ radius ratio geometry.

It may be seen that the pressure levels at the outlet region are increased as λ increases. However, the pressure at inlet and at the mid of the vaned region decreases with λ increases, indicating that there is a pressure loss region at the vaneless annular passage. This is known a source of losses as mentioned in Aungier's work (Aungier, 2000). When comparing λ = 1.2 and λ = 1.1 it is possible to notice that the pressure recovery presents better behavior, since the throat phenomena is mitigated and thus the pressure recovery is benefited, and the pressure levels at the vane outlet region are higher. In conclusion, the pressure contours indicates that there is a balance between pressure losses at vaneless annular passage and pressure losses at the vane throat region, which explains the optimal behavior at λ = 1.2. This final consideration is reinforced when observing λ = 1.2 and λ = 1.3, since the first one does have lower pressure levels at vane outlet region, however, its counterpart presents bigger pressure loss region at the vaneless annular passage, jeopardizing pressure recovery and thus the efficiency level.

4. CONCLUSION

In conclusion, this study examined the performance parameters of a centrifugal compressor, focusing on isentropic efficiency, pressure recovery, and required power. The analysis revealed interesting trends and raised questions that require further investigation.

It was observed that the vaneless annular passage, primarily controlled by the λ Leading edge - Impeller outlet radius ratio, significantly impacts the compressor's performance levels, as indicated by changes in Efficiency levels presented in Figure 4. With an optimal value of 82.6% at λ = 1.2.

However, the other performance parameters had no significant alterations, with pressure ratio changing in order of 1%, same order that the grid variation error, and required power changing in order of 0.04%, which is lower than the grid variation error.

Observing the post-processed simulation results, it is possible to conclude that the optimal case presented lower recirculation zones, maintained the flow guidance, presented lower throat zones and had higher pressure levels at vane outlet regions while maintaining similar vaneless annular passage pressure behavior. This led to reasonable assumptions that the vaneless annular passage can impact the flow and led to flow phenomena responsible for efficiency impacts.

The λ radius ratio variation in this analysis caused a change in the vane's shape, which is pronounced at $\lambda = 1.4$ and presented no recirculation zones but poor guidance characteristics, jeopardizing the efficiency level.

Since an optimal value is observed at $\lambda = 1.2$, it is reasonable to conclude that redesigning the vaneless annular passage would be a beneficial practice for the designer. However, it is important to acknowledge that the vaneless annular passage is just one of the factors and is a region of the vaned diffuser component. Other important factors should also be considered. Therefore, further investigations are required to comprehend the underlying flow phenomena and explain some of the observed tendencies.

While there is still more to study, it is worth noting that this analysis would not have been possible solely using classical 1-D techniques, highlighting the advantages of employing 3D-CFD simulations coupled with 1D analysis software to generate preliminary geometries in centrifugal machines analysis.

5. REFERENCES

Ameli, A., Afzalifar, A., Turunen-Saaresti, T., & Backman, J., 2019. *Centrifugal compressor design for near-critical point applications.* Journal of Engineering for Gas Turbines and Power, 141(3). https://doi.org/10.1115/1.4040691

Aungier, R. H., 2000. *Centrifugal compressors: a strategy for aerodynamic design and analysis.* ASME Press.

Bell, I. H., Wronski, J., Quoilin, S., & Lemort, V., 2014. *Pure and pseudo-pure fluid thermophysical property evaluation and the open source thermophysical property library coolprop*. Industrial and Engineering Chemistry Research, 53(6), 2498–2508. https://doi.org/10.1021/ie4033999

Casey, M., & Robinson, C., 2012. *A Method to Estimate the Performance Map of a Centrifugal Compressor Stage*. Journal of Turbomachinery, 135(2). https://doi.org/10.1115/1.4006590

Casey, M., & Robinson, C., 2021. *Radial Flow Turbocompressors: Design, Analysis and Applications*. Cambridge University Press.

Celik, I. B., Ghia, U., Roache, P. J., Freitas, C. J., Coleman, H., & Raad, P. E., 2008. *Procedure for estimation and reporting of uncertainty due to discretization in CFD applications.* Journal of Fluids Engineering, Transactions of the ASME, 130(7), 0780011–0780014. https://doi.org/10.1115/1.2960953

De Wet, A. L., Von Backström, T. W., Backström, B., & Van Der Spuy, S. J., 2012. *Performance investigation of a turbocharger compressor*. http://www.asme.org/about-asme/terms-of-use

Denton, J. D., 1993. *The 1993 IGTI Scholar Lecture Loss Mechanisms in Turbomachines.* http://www.asme.org/terms/Terms_Use.cfm

Godec, M., Kuuskraa, V., Van Leeuwen, T., Melzer, L. S., & Wildgust, N., 2011. *CO2 storage in depleted oil fields: The worldwide potential for carbon dioxide enhanced oil recovery.* Energy Procedia, 4, 2162–2169. https://doi.org/10.1016/j.egypro.2011.02.102

Hosangadi, A., Liu, Z., & Weathers, T., 2018. *Numerical Simulations of CO2 Compressors: Subcritical Inlet Conditions.*

Kim, S., 2020. *The effects of foreign direct investment, economic growth, industrial structure, renewable and nuclear energy, and urbanization on Korean greenhouse gas emissions.* Sustainability (Switzerland), 12(4). https://doi.org/10.3390/su12041625

Lee, Y.-T., Luo, L., & Bein, T. W., 2000. *Direct method for optimization of a centrifugal compressor vaneless diffuser.* http://proceedings.asmedigitalcollection.asme.org/pdfaccess.ashx?url=/data/conferences/asmep/80301/

Menter, F. R., 1994. *Two-equation eddy-viscosity turbulence models for engineering applications.* AIAA Journal, 32(8), 1598–1605. https://doi.org/10.2514/3.12149

Niu, Z., Sun, Z., Wang, B., & Zheng, X., 2022. *Effects of Nonaxisymmetric Volute on Rotating Stall in the Vaneless Diffuser of Centrifugal Compressors.* Journal of Engineering for Gas Turbines and Power, 144(5). https://doi.org/10.1115/1.4053389

Roddy, Dermot., 2010. *Advanced power plant materials, design, and technology.* Woodhead Pub.

Shaaban, S., 2015. *Design optimization of a centrifugal compressor vaneless diffuser.* International Journal of Refrigeration, 60, 142–154. https://doi.org/10.1016/j.ijrefrig.2015.06.020

Sorokes, J. M., & Jim, J. M. "., 2018. *Centifugal compressor evolution.* 47th Turbomachinery & 34th Pumo symposia. Houston, Texas | September 17-20, 2018.

6. RESPONSIBILITY NOTICE

The authors are the only responsible for the printed material included in this paper.